

Examining ambient noise using co-located measurements of rotational and translational motion

Céline Hadziioannou · Peter Gaebler · Ulrich Schreiber · Joachim Wassermann · Heiner Igel

Received: date / Accepted: date

Abstract In the past decade a number of studies have reported the observation of rotational motion associated with seismic events. We report a first observation of rotational motion in the microseismic ambient noise band. A striking feature of rotational motion measurements is that the information about the seismic phase velocity and source backazimuth is contained in the amplitude ratio of a point measurement of rotation rate and transverse acceleration. We investigate the possibility of applying this method to ambient noise measured with a ring laser and a broadband seismometer at the Wettzell geodetic observatory in Germany. Using data in the secondary microseismic band, we recover local phase velocities as well as the backazimuth of the strongest noise source for two different time periods. In order to confirm these findings we additionally compare the results with classical array processing techniques of the nearby located Gräfenberg array.

C. Hadziioannou · H. Igel · J. Wassermann
Department of Earth and Environmental Sciences
Ludwig-Maximilians-Universität
Theresienstr. 41
80333 Munich, Germany
E-mail: hadzii@geophysik.uni-muenchen.de

P. Gaebler
Sektion 2.4 Seismologie
Helmholtz-Zentrum Potsdam
Deutsches GeoForschungsZentrum GFZ
Telegrafenberg, 14473 Potsdam, Germany

U. Schreiber
Forschungseinrichtung Satellitengeodäsie
Fundamentalstation Wettzell
Sackenriederstrasse 25
93444 Bad Kötzing, Germany

1 Introduction

To fully describe the seismic wave field one needs to measure three components of translational motion, six components of strain and three components of rotational motion (Aki and Richards, 2002). The use of seismometers and strainmeters to measure translational motion and strain, respectively, has been established for decades (e.g. Alsop et al (1961); Gombert and Agnew (1996)). On the other hand, instruments suitable for measuring rotational motions are only starting to make their appearance. In particular, the development of high sensitivity ring laser gyroscopes has made it possible to detect rotational motions excited by seismic events (Stedman et al, 1995; McLeod et al, 1998; Pancha et al, 2000).

One interesting property is that, assuming plane wave propagation, the amplitude ratio of rotational motion around a vertical axis, and the transverse acceleration is twice the horizontal phase velocity (Pancha et al, 2000; Igel et al, 2005; Ferreira and Igel, 2009). Kurrle et al (2010) have shown the possibility and associated difficulties of determining local Love wave dispersion curves using such co-located measurement of both types of ground motion resulting from several seismic events. Igel et al (2007) used the same method to determine the backazimuth of a seismic event, as well. This paper concentrates on the application of the method to ambient noise. We study the origin of oceanic noise sources using two methods: amplitude ratios of co-located measurements of translational and rotational motions recorded at Wettzell, Germany (Schreiber et al, 2009), and classical $f - k$ analysis using the Gräfenberg array.

Previously, McLeod et al (1998) and Pancha et al (2000) have shown that ring laser gyroscopes provide sufficient accuracy to measure seismically induced ground

rotations. However, for this study it is important to determine if the Wettzell ring laser is sufficiently sensitive to continually detect ambient seismic noise. In section 2 we characterize the noise level of the Wettzell ring laser. Sections 3 and 4 detail the theory and processing applied, respectively. In section 5, we determine the noise source direction using only co-located rotational and translational measurements, for two different time periods. The reliability of these results is then assessed using independent array analysis in section 6.

2 Characterization of Noise on Wettzell Ring Laser

Most ambient noise in the periods from 5 to 20 seconds is generated by the interaction of the atmosphere, ocean waves and the ground. The spectrum of this oceanic noise is dominated by two peaks, the primary microseismic peak at a period around 14 seconds, and the secondary microseismic peak around 7 seconds (e.g. Friedrich et al (1998)). Longuet-Higgins (1950) suggests that the primary microseismic peak originates directly from forces on the sea floor induced by strong oceanic waves. The stronger secondary microseisms are believed to result from nonlinear interaction of these waves, producing the double-frequency peak. In both cases, the microseismic noise is dominated by fundamental mode surface waves, with Rayleigh waves contributing four times as much energy as Love waves in the secondary microseismic band (Friedrich et al, 1998).

Numerous past studies have attempted to localize the origin of primary and secondary microseisms (e.g. Gutenberg (1947); Cessaro (1994); Landès et al (2010)). In this study, we attempt to determine the backazimuthal direction of the strongest microseismic source using co-located rotational motion and transverse acceleration measurements.

This study uses rotational motions recorded at the ring laser of the Wettzell geodetic observatory in Germany (see figure 1). Ring lasers are active interferometers, where a polygon cavity is used in both directions to generate a spectrally narrow laser beam. Depending on the experienced rotation by the entire apparatus, these two counter-propagating laser beams differ slightly in optical frequency. Beating the two light beams against each other yields an interferogram, which is strictly proportional to the experienced rate of rotation. The lower the loss of the mirrors, the smaller is the linewidth of the laser function and consequently the higher the resolution of the sensor. In 2009, the ring laser was upgraded with fused silica mirrors for which a superior polish can be achieved, which improved the gyroscope performance.

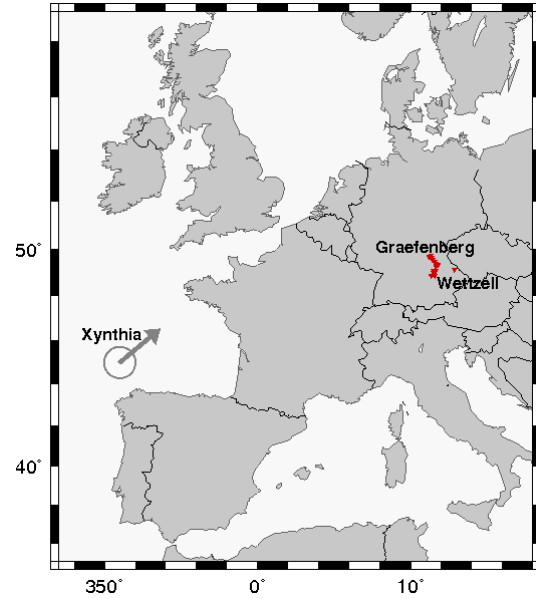


Fig. 1 Location of Gräfenberg seismic array and the Wettzell geodetic observatory. Stations WET and RLAS are located at the latter. The location of the Xynthia storm on February 27, 2010 as well as its direction are indicated by the circle and arrow (see also section 5).

To establish if oceanic microseisms can be detected with this instrument, first its overall noise level is studied. We characterize the noise recorded on the Wettzell ring laser (RLAS) using the method described in McNamara and Buland (2004). In this method, a statistical analysis is performed on power spectral densities (PSD) taken of 1-hour segments of noise. The analysis yields the probability density function of the noise power as a function of frequency for each station component.

In order to compare the noise level before and after the instrument improvement in 2009, two months of continuous recordings in the quiet summer periods of 2008 and 2010 were used. The top curve in figure 2 represents the background noise power before the mirror upgrade, the bottom curve represents the same afterwards. The flat behavior of the top curve is in agreement with the results by Widmer-Schmidrig and Zürn (2009), and is most likely due to instrument noise, not ambient seismic noise.

Figure 2 shows that the overall instrument noise level on the Wettzell ring laser decreased by 20 dB after the instrument upgrade, which corresponds to a factor 10 in amplitude. After 2009 (bottom curve), an elevated noise level with respect to the mostly flat instrument noise is visible in the $[0.1 \text{ } 0.2]\text{Hz}$ range demonstrates that the Wettzell ring laser is capable of detecting ambient noise in the secondary microseismic peak. The detection of ambient noise in the primary microseismic peak ($[0.05 \text{ } 0.1]\text{Hz}$) is more ambiguous. The reasons

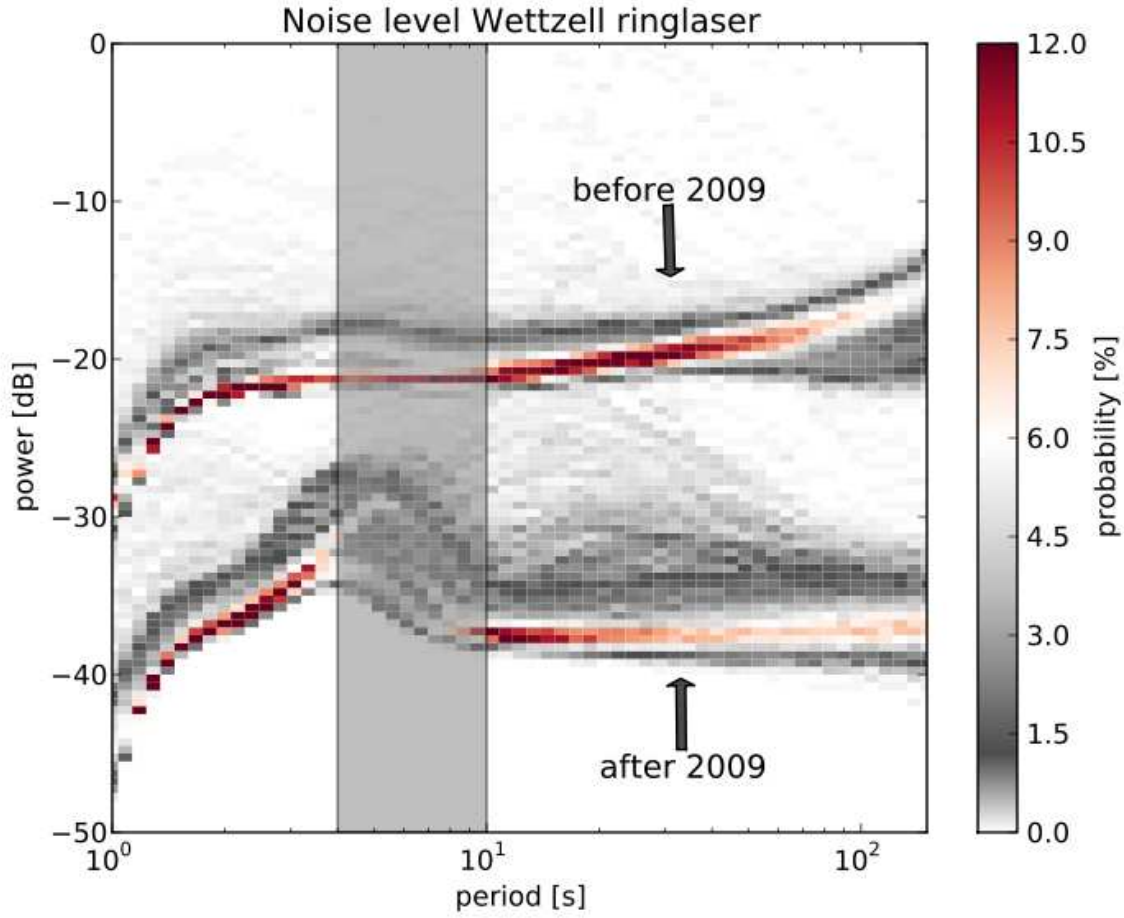


Fig. 2 Wettzell ring laser noise level relative to $1(\text{nrad/s})^2/\text{Hz}$ *before* (top curve) and *after* (bottom curve) an instrument improvement in 2009 (after McNamara and Buland (2004)). Noise levels determined during the summer months of 2008 and 2010, respectively. The colorscale indicates the probability of measuring a certain noise level, the grey shading corresponds to the secondary microseismic band.

for this different detection level are the significantly higher amplitudes excited by the secondary microseisms in comparison to the primary microseisms, making the first easier to observe (Berger et al, 2004).

Since we have established that the Wettzell ring laser detects the secondary microseisms, the analysis in the next sections will concentrate on the corresponding frequency band ($[0.1 \text{ } 0.2]\text{Hz}$).

3 Theory

For a horizontally polarized plane wave propagating in a homogeneous medium, the similarity between co-located measurements of vertical rotation rate ($\dot{\omega}_z$) and transverse acceleration (a_T) is expected to be maximal. The displacement field for an incident wave, transversely polarized along the y-axis, is defined as:

$$\mathbf{u} = [0, A \sin(kx - kct), 0] \quad (1)$$

with amplitude A , wavenumber k , phase velocity c and radian frequency ω . The displacement field \mathbf{u} and rotational motions ω are related by:

$$\omega = \begin{pmatrix} \omega_x \\ \omega_y \\ \omega_z \end{pmatrix} = \frac{1}{2} \nabla \times \mathbf{u} = \frac{1}{2} \begin{pmatrix} \partial_y u_z - \partial_z u_y \\ \partial_z u_x - \partial_x u_z \\ \partial_x u_y - \partial_y u_x \end{pmatrix} \quad (2)$$

The rotation rate around a vertical axis $\dot{\omega}_z$ is then given by:

$$\dot{\omega}_z = \frac{1}{2} k^2 c A \sin(kx - kct), \quad (3)$$

while the transverse acceleration is given by:

$$a_T = \ddot{u}_T = -k^2 c^2 A \sin(kx - kct). \quad (4)$$

From equations (3) and (4), the ratio between the transverse acceleration and the vertical rotation rate is:

$$\frac{a_T}{\dot{\omega}_z} = \frac{-k^2 c^2 A \sin(kx - kct)}{\frac{1}{2} k^2 c A \sin(kx - kct)} = -2c \quad (5)$$

This simple relation means that we can estimate phase velocities from the amplitude ratio co-located measurements of rotational and translational motions.

From equation (5) we can also see that the two signals should have the same waveform, save for the $-2c$ factor. This property can be used to estimate the source direction of SH-type motions by rotating the horizontal components of the seismometer record along different angles, until their resemblance with the rotational measurements is maximal. The corresponding angle will then point in the direction of the source. Igel et al (2007) and Kurrle et al (2010) have applied this analysis to seismic events. In the next section, it will be applied to ambient noise in the secondary microseismic band.

4 Processing

The rotational motion around the vertical axis ($\dot{\omega}_z$) is measured with the Wettzell ring laser (RLAS), while the translational ground motion is measured with a STS2 broadband seismometer at the German Regional Seismic Network (GRSN) station WET (see figure 1). This seismometer is located less than 260 meters from the ring laser, and can thus be considered as co-located with the ring laser for the frequency range investigated in this study.

The seismometer velocity records are corrected for instrument response and differentiated to obtain the acceleration. The records from the ring laser only need to be divided by a frequency-independent gain factor to obtain the rotation rate. Finally, all signals are band-pass filtered using a fourth order Butterworth filter in the secondary microseismic band: [0.1 0.2]Hz. All processing is done with the ObsPy toolbox (Beyreuther et al, 2010; Megies et al, 2011).

According to equation (5) the amplitude ratio of transverse acceleration and vertical rotation rate gives the apparent phase velocity. The backazimuth of the source can also be determined by rotating the horizontal components of the transverse acceleration until the similarity with the vertical rotation rate signal is maximal.

First, a backazimuth vector is defined with evenly distributed angles between 0 and 360 degrees. The transversal acceleration a_T is then obtained for each backazimuth angle θ_i by rotating the horizontal acceleration components. The similarity between the transversal acceleration and the rotation rate is quantified by calculating the cross-correlation coefficient, which is defined between 0 for no similarity and 1 for a perfect match. The backazimuth angle for the best-fitting transverse acceleration points in the direction of the source.

This process is repeated for a number of overlapping, moving time windows along the signal, in order to follow the evolution of the main source orientation. The time window length is fixed at a few times the central period T_c . For each 60 second window, for which the cross-correlation coefficient between the two signals exceeds a threshold which we set at 0.75, the phase velocity is estimated according to equation 5. This is done by finding the optimal scaling between the rotation rate and the best-fitting transverse acceleration, according to a least squares method.

In the following section, this procedure is tested on a seismic event with known backazimuth, as well as on a day with a strong microseismic source.

5 Results

First of all the amplitude ratio method is tested on a seismic event, using two frequency bands: the first excluding oceanic microseisms ([0.01 0.03]Hz, figure 3), the second centered on the secondary microseismic peak ([0.1 0.2]Hz, figure 4). On March 11, 2011, the $M_W 9.0$ Tohoku-Oki event occurred at 05:46 UTC, with a theoretical backazimuth of 37° relative to Wettzell station. Figures 4b and 3b show the cross-correlation coefficient between rotational and transverse measurements as a function of backazimuth and time. In figure 3, with the microseismic frequency bands excluded, the waveform cross-correlation exceeds the threshold value of 0.75 only at the times of the main event and subsequent aftershocks. The correlation coefficient at those times reaches a maximum at the theoretical backazimuth of the event (red dashed line), which indicates that the method works for seismic events. The apparent phase velocities attain realistic values as well, of the order of 12 km/s for a steep incidenting S-wave arrival, then dropping to values around 4 km/s, which corresponds well to theoretical Love wave phase velocities.

When the frequency band is centered on the secondary microseismic peak (figure 4), the waveform correlation stays high throughout the day, even in absence of any seismic events. At times without seismic events, the maximum of the correlation coefficient consistently lies at a backazimuth of 300° . This suggests that we are observing a microseismic noise source with a backazimuth of 300° . This observation is supported by the work of Darbyshire (1991) and Friedrich et al (1998), who both find a source of secondary microseismic noise in the Channel region.

The results using data with a major seismic event are promising, and even seem to show a consistent microseismic source. To test if ambient noise source directions can be found, the method is tested on a time

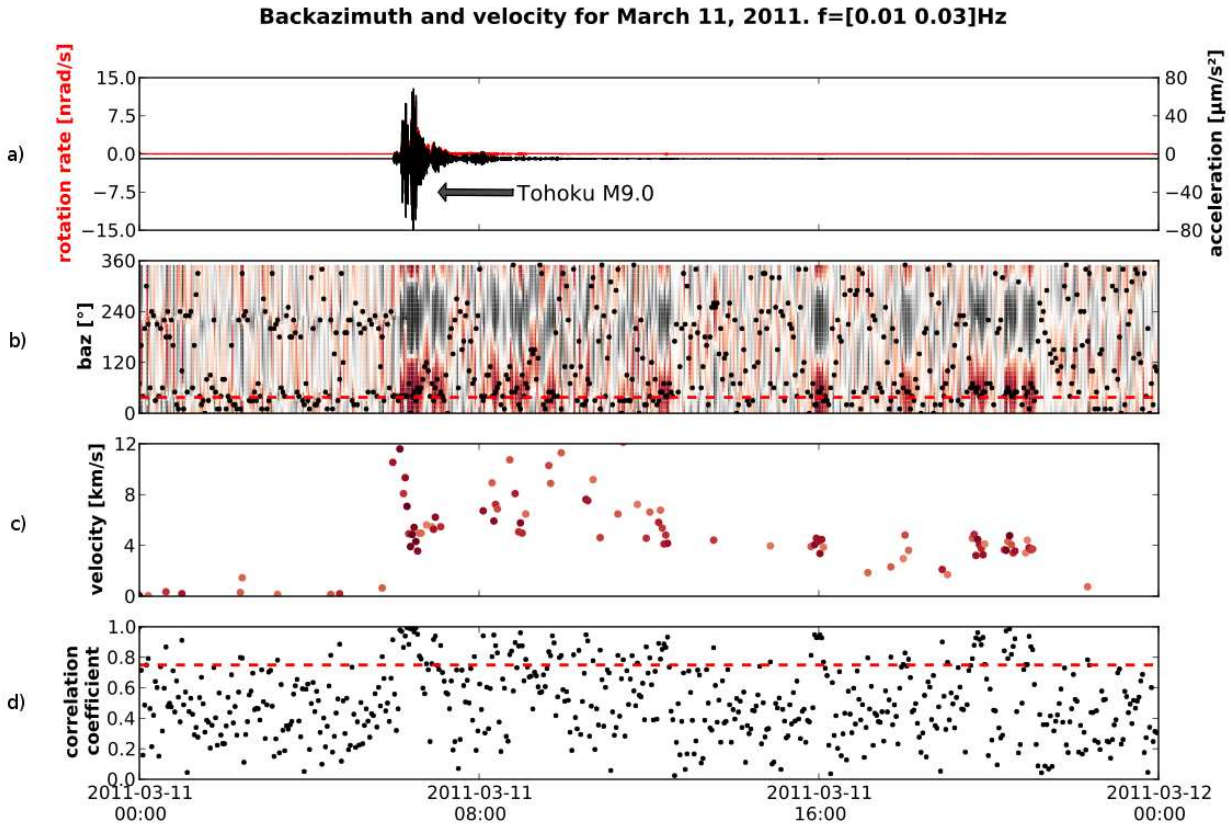


Fig. 3 Data for March 11, 2011, with the $M_W 9.0$ Tohoku-Oki event at a backazimuth of 37° . (a) Traces for rotation rate in red and transverse acceleration in black. (b) Backazimuth, with colorscale indicating the cross-correlation coefficient for each backazimuth, where red is positive high and black negative high. A black dot marks the maximum correlation coefficient. Median backazimuth is indicated by a white line, the theoretical backazimuth of the Tohoku-Oki event by a dashed red line. (c) Phase velocity obtained from amplitude ratio ($\frac{a_T}{\omega_r}$), colorscale corresponds to the correlation coefficient as in (b). (d) Maximum correlation coefficient between rotation rate and transverse acceleration. The red dashed line indicates the threshold value of 0.75. Frequency band $f = [0.01 \ 0.03]$ Hz excludes the secondary microseismic peak.

period with a strong acting source of oceanic noise at a known location. On February 26, 2010, the Xynthia storm originated 30° off the coast west of Portugal (see figure 1). A high energy low pressure system like the Xynthia storm significantly increases the height of ocean waves while it is on the open sea or near coast-lines. Such increased waveheight is directly linked to the generation of primary and secondary microseismic noise. This particular storm generated strong microseismic activity at a backazimuth of around 260° with respect to Wettzell. In addition to this, on the same date a seismic event occurred in Japan ($M_W 7.0$ Ryukyu event), with a theoretical backazimuth of around 45° .

Figure 5 shows the signals for vertical rotation rate and transverse acceleration, the apparent phase velocity obtained using amplitude ratios, the cross-correlation coefficient for each backazimuth as a colorscale and finally the maximum correlation coefficient. Over the course of the day, a maximum cross-correlation coefficient

(fluctuating around 0.8) is found at a backazimuth of $\sim 270^\circ$. This corresponds roughly to the South-Western direction, and matches the expected backazimuth of the Xynthia storm (260°) closely. In addition to this, the correlation coefficient briefly reaches a maximum value for a backazimuth of $\sim 50^\circ$ at the time of the Ryukyu event.

Note the higher amplitudes of the ring laser measurement starting around 17:00. These fluctuations correlate with high wind speeds measured at the meteorological station in Wettzell. There are two possible phenomena at work here. First, strong wind gusts may cause a tilting effect on the ring laser system, which in turn can affect the measured rotation rate. However, Pham et al (2009) showed, that this effect is negligible in the case of strong teleseismic events and therefore is likely very small in the case of wind influence as well. A second cause can be modeled by shear forces on the building excited by strong local acting wind. These

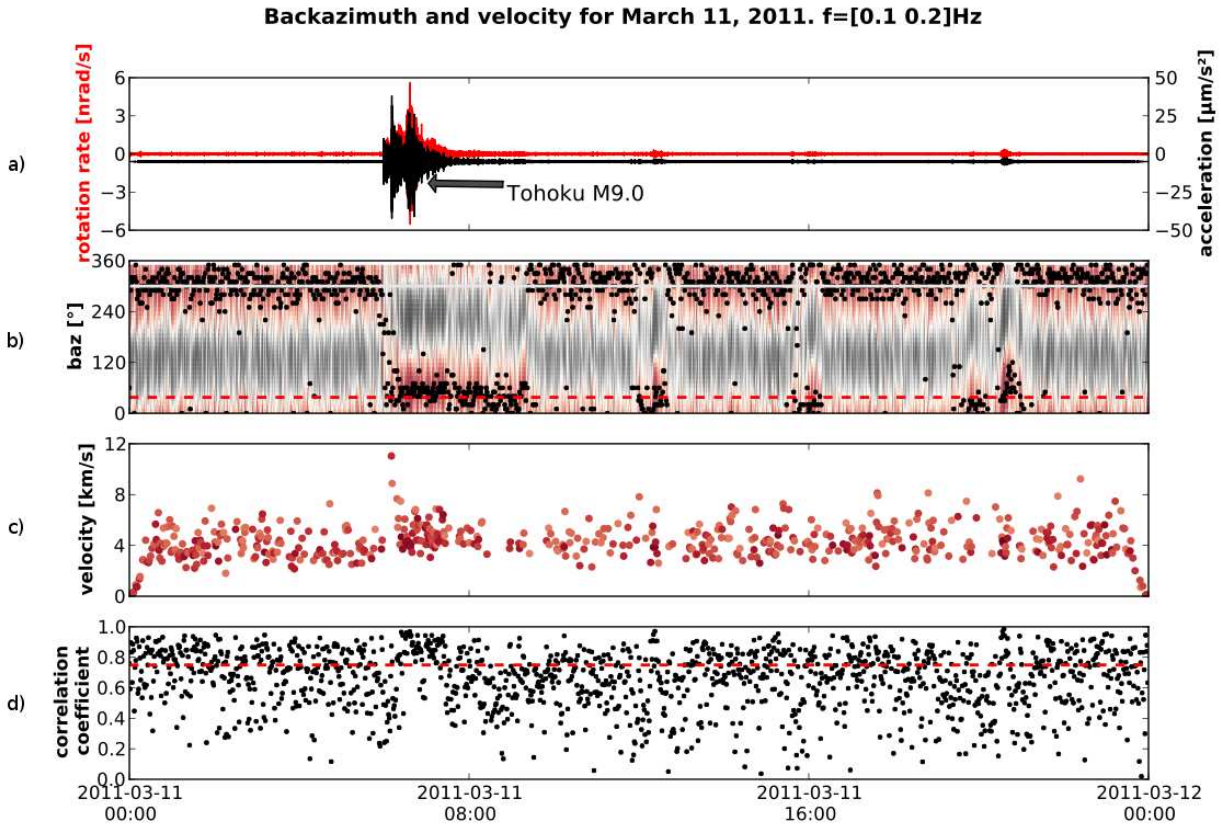


Fig. 4 As figure 4, but for $f = [0.1 \ 0.2]\text{Hz}$, including the secondary microseismic peak.

shear forces may be transmitted to the ring laser system and thus cause significant variations in the measured rotation rate. This sensitivity of the Wettzell ring laser to local wind speeds does not affect the results in this study, as the consequent decrease of cross-correlation coefficient disqualifies the affected time windows. However, it is important to be aware of this effect.

The results in this section give strong evidence that it is possible to find the direction and apparent phase velocity not only of seismic events, but of ambient noise sources as well, using only a point measurement. In the next section, we confirm the observations with an independent analysis using classic array processing methods.

6 Comparison to $f - k$ Analysis

Following the promising results in the previous section, a frequency-wavenumber analysis is performed using data from the Gräfenberg seismic array (see figure 1) for both time periods analysed in section 5. This array consists of 13 3-component broadband stations and is located about 50 km west of the Wettzell station (see

figure 1). The aperture of the array and the average interstation distance make it suitable to study the microseismic band. Since the array is close to the Wettzell station, we can assume that the same noise sources are observed at both locations. Sources of ambient noise Rayleigh waves are believed to be at approximately the same locations as those of Love waves (Nishida et al (2008)). Therefore, only vertical component records are used in the array analysis.

The data from the Gräfenberg stations are corrected for instrument response, and bandpass filtered for $[0.1 \ 0.2]\text{Hz}$ using a fourth order Butterworth filter. Next, frequency-wavenumber analysis is performed for a moving time window. The length of the time window is taken such that more than one wavelength of the slowest waves is recorded over the whole array. The beam-power maximum is picked for each time window, and its backazimuth is represented in figure 6. The backazimuths found using the amplitude ratio method described in section 3 are indicated in the figures as a black dashed line. At both dates, consistent noise sources are detected at backazimuths of $270^\circ - 280^\circ$, respectively. As in figure 4, the backazimuth found in figure 6

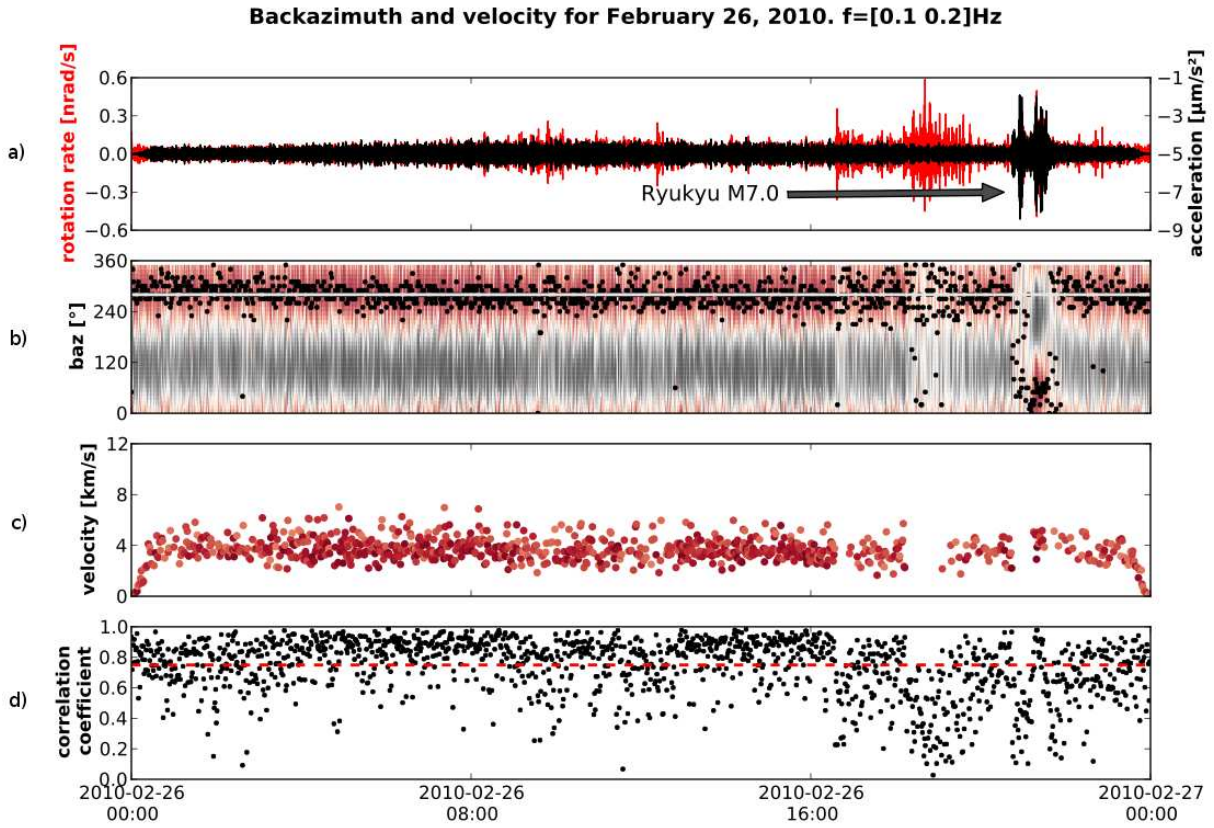


Fig. 5 One day of data during the Xynthia storm (February 26, 2010). Event is the $M_W 7.0$ Ryukyu event with a backazimuth of 45° . (a) Traces for rotation rate in red and transverse acceleration in black. (b) Backazimuth, with colorscale indicating the cross-correlation coefficient for each backazimuth, where red is positive high and black negative high. A black dot marks the maximum correlation coefficient. Median backazimuth is indicated by a white line. (c) Phase velocity obtained from amplitude ratio ($\frac{a_T}{\omega_z}$), colorscale corresponds to the correlation coefficient as in (b). (d) Maximum correlation coefficient between rotation rate and transverse acceleration. The red dashed line indicates the threshold value of 0.75. $f = [0.1 \ 0.2]\text{Hz}$

temporarily shifts to the direction of the Tohoku-Oki event and its aftershocks.

The excellent agreement with the results from classic frequency-waveform analysis proves that it is possible to determine the ambient noise source orientation using only a co-located measurement of rotation rate and transverse acceleration.

7 Discussion and Conclusion

Recently, improved sensitivity of sensors have made it possible to observe rotational ground motions induced by seismic events. However, the consistent observation of rotational motions in ambient noise has proven difficult. We have shown that, as a result of the instrument improvement in 2009, the Wettzell ring laser can detect rotational motions in microseisms in the secondary microseismic band ($[0.1 \ 0.2]\text{Hz}$).

A co-located measurement of rotation rate and transverse acceleration lead to a backazimuth estimation as well as one for the apparent phase velocity. By applying the method detailed in section 3, a consistent high correlation between rotation rate and transverse acceleration signals is found in the secondary microseismic band, which is not present at different frequencies. This high correlation points to a noise source at a backazimuth of 300° . Testing the same method with a different data set including a date with a strong noise source (the Xynthia storm) yields a backazimuth close to the theoretical value of $\sim 270^\circ$. The apparent velocities found with this method correspond to the expected local values.

Finally, these results are checked against classic array beamforming analysis. For practical reasons, this $f - k$ analysis was performed on vertical component records and thus using mainly Rayleigh waves. However, since both ambient noise Rayleigh and Love waves are believed to be generated in the same areas (Nishida

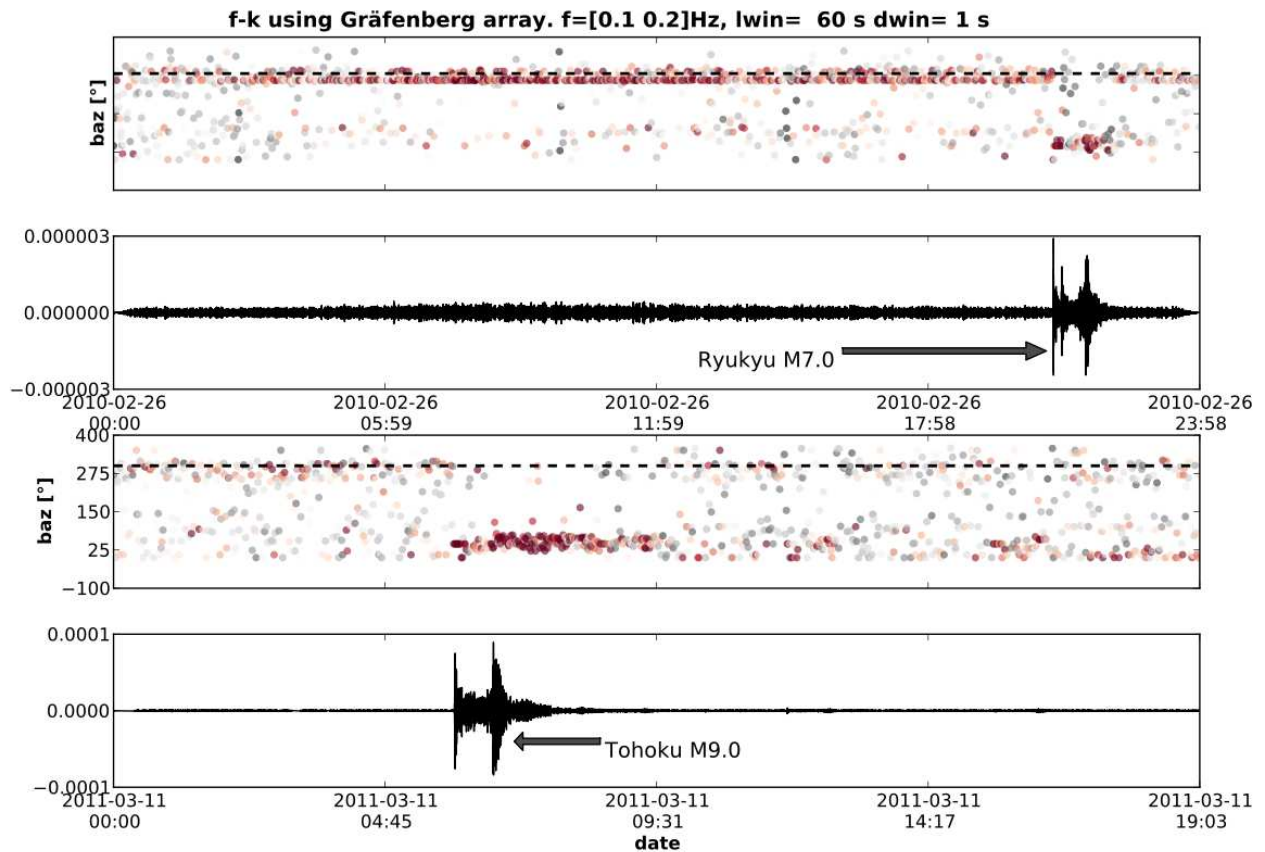


Fig. 6 Frequency-wavenumber analysis on the Z-component of the Gräfenberg array. Top: during the Xynthia storm (February 26, 2010). Event is the M_W 7.0 Ryukyu event. Bottom: during the M_W 9.0 Tohoku-Oki event (March 11, 2011). Backazimuth - value obtained for microseismic signal with the amplitude ratio ($\frac{a_x}{a_z}$) indicated by a dashed black line, colorscale indicates the beampower, with red high and black low. Signals are recorded at station GRA1. $f = [0.1 \ 0.2]\text{Hz}$.

et al (2008)), the results can still be compared. Using array beamforming techniques, the same main source backazimuths are found as with the amplitude ratio method in section 5.

Acknowledgements We gratefully acknowledge support from the European Commission (Marie Curie Actions, ITN QUEST, www.quest-itn.org). We also acknowledge support from the German Research Foundation (project Ig16-8).

References

- Aki K, Richards P (2002) Quantitative seismology, second edition. University Science Books
- Alsop L, Sutton G, Ewing M (1961) Free oscillations of the earth observed on strain and pendulum seismographs. *J Geophys Res* 66(2):631–641
- Berger J, Davis P, Ekström G (2004) Ambient earth noise: a survey of the global seismographic network. *Geophys Res Lett* 109:B11,307
- Beyreuther M, Barsch R, Krischer L, Megies T, Behr Y, Wassermann J (2010) Obspy: A python toolbox for seismology. *Seis Res Lett* 81(3):530
- Cessaro R (1994) Sources of primary and secondary microseisms. *Bull Seismol Soc Am* 84(1):142
- Darbyshire J (1991) A further investigation of microseisms recorded in north wales. *Phys Earth Planet Inter* 67(3-4):330–347
- Ferreira A, Igel H (2009) Rotational motions of seismic surface waves in a laterally heterogeneous earth. *Bull Seismol Soc Am* 99(2B):1429
- Friedrich A, Krüger F, Klinge K (1998) Ocean-generated microseismic noise located with the gräfenberg array. *Journal of Seismology* 2(1):47–64
- Gomberg J, Agnew D (1996) The accuracy of seismic estimates of dynamic strains: An evaluation using strainmeter and seismometer data from pinon flat observatory, california. *Bull Seismol Soc Am* 86(1A):212
- Gutenberg B (1947) Microseisms and weather forecasting. *Journal of Meteorology* 4(1):21–28

- Igel H, Schreiber U, Flaws A, Schuberth B, Velikoseltsev A, Cochard A (2005) Rotational motions induced by the m8. 1 tokachi-oki earthquake, september 25, 2003. *Geophys Res Lett* 32:L08,309
- Igel H, Cochard A, Wassermann J, Flaws A, Schreiber U, Velikoseltsev A, Pham Dinh N (2007) Broad-band observations of earthquake-induced rotational ground motions. *Geophys J Int* 168(1):182–196
- Kurrle D, Igel H, Ferreira AMG, Wassermann J, Schreiber U (2010) Can we estimate local Love wave dispersion properties from collocated amplitude measurements of translations and rotations? *Geophys Res Lett* 37(4):1–5,
- Landès M, Hubans F, Shapiro NM, Paul A, Campillo M (2010) Origin of deep ocean microseisms by using teleseismic body waves. *J Geophys Res* 115(B5):1–14
- Longuet-Higgins M (1950) A theory of the origin of microseisms. *Philosophical Transactions of the Royal Society of London Series A Mathematical and Physical Sciences* 243(857):1–35
- McLeod D, Stedman G, Webb T, Schreiber U (1998) Comparison of standard and ring laser rotational seismograms. *Bull Seismol Soc Am* 88(6):1495
- McNamara DE, Buland RP (2004) Ambient Noise Levels in the Continental United States. *Bull Seismol Soc Am* 94(4):1517–1527
- Megies T, Beyreuther M, Barsch R, Krischer L, Wassermann J (2011) Obspy—what can it do for data centers and observatories? *Annals of Geophysics* 54(1):47–58
- Nishida K, Kawakatsu H, Fukao Y, Obara K (2008) Background Love and Rayleigh waves simultaneously generated at the Pacific Ocean floors. *Geophys Res Lett* 35(16):1–5
- Pancha A, Webb TH, Stedman GE, McLeod DP, Schreiber KU (2000) Ring laser detection of rotations from teleseismic waves. *Geophys Res Lett* 27(21):3553
- Pham N, Igel H, Wassermann J, Kaser M, de La Puente J, Schreiber U (2009) Observations and modeling of rotational signals in the p coda: constraints on crustal scattering. *Bull Seismol Soc Am* 99(2B):1315
- Schreiber K, Hautmann J, Velikoseltsev A, Wassermann J, Igel H, Otero J, Vernon F, Wells J (2009) Ring laser measurements of ground rotations for seismology. *Bull Seismol Soc Am* 99(2B):1190
- Stedman G, Li Z, Bilger H (1995) Sideband analysis and seismic detection in a large ring laser. *Applied Optics* 34(24):5375–5385
- Widmer-Schmidrig R, Zürn W (2009) Perspectives for ring laser gyroscopes in low-frequency seismology. *Bull Seismol Soc Am* 99(2B):1199